Science of the Total Environment 817 (2022) 152741

Contents lists available at ScienceDirect

Science of the Total Environment

journal homepage: www.elsevier.com/locate/scitotenv

Interaction of hyperaccumulating plants with Zn and Cd nanoparticles

Davide Imperiale [a,b,c], Giacomo Lencioni [a], Marta Marmiroli [a], Andrea Zappettini [d], Jason C. White [e], Nelson Marmiroli [a,b,*]

[a] Department of Chemistry, Life Sciences and Environmental Sustainability, University of Parma, Parma, Italy
[b] National Interuniversity Consortium for Environmental Sciences (CINSA), Parma, Italy
[c] Interdepartmental Center Siteia Parma, University of Parma, Parma, Italy
[d] IMEM-CNR Istituto dei Materiali per l'Elettronica ed il Magnetismo, Parma, Italy
[e] The Connecticut Agricultural Experiment Station, New Haven, CT, USA

HIGHLIGHTS

- Here is a first evidence plants hyperaccumulating ENP (Zn QDs and Cd QDs).
- This occurs in medium supplemented with non-toxic amounts of ENP without significant disrupting of ENP.
- Hyperaccumulation of ENP was showed by BCF and TF similar when to those from Zn and Cd salts.
- Hyperaccumulation of ENP may involve their biotransformation with formation of ionic metal but a portion of ENP remains.
- This constitute new possibilities of searching for Zn and Cd ENP hyperaccumulator with greater phytoremediation potential.

GRAPHICAL ABSTRACT

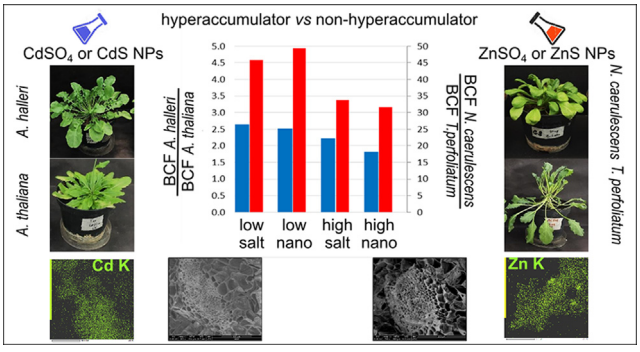

ARTICLE INFO

Article history:
Received 25 May 2021
Received in revised form 23 December 2021
Accepted 24 December 2021
Available online 3 January 2022

Editor: Charlotte Poschenrieder

Keywords:
Nanoscale metals
Uptake and translocation
Hyperaccumulation
A. helleri
N. caerulescens
TEM/ESEM

ABSTRACT

Metal hyperaccumulating plant species are an interesting example of natural selection and environmental adaptation but they may also be useful to developing new technologies of environmental monitoring and remediation. *Noccaea caerulescens* and *Arabidopsis halleri* are both Brassicaceae and are known metal hyperaccumulators. This study evaluated tolerance, uptake and translocation of zinc sulfide quantum dots by *N. cearulescens* and cadmium sulfide quantum dots by *A. halleri* in direct comparison with the non-hyperaccumulator, genetically similar *T. perfoliatum* and *A. thaliana*. Growth media were supplied with two different concentrations of metal in either salt ($ZnSO_4$ and $CdSO_4$) or nanoscale form (ZnS QDs and CdS QDs). After 30 days of exposure, the concentration of metals in the soil, roots and leaves was determined. Uptake and localization of the metal in both nanoscale and non-nanoscale form inside plant tissues was investigated by Environmental Scanning Electron Microscopy (ESEM) equipped with an X-ray probe. Specifically, the hyperaccumulators in comparison with the non-hyperaccumulators accumulate ionic and nanoscale Zn and Cd in the aerial parts with a BCF ratio of 45.9 for Zn ion, 49.6 for nanoscale Zn, 2.64 for Cd ion and 2.54 for nanoscale Cd. Results obtained with a differential extraction analytical procedure also showed that a significant fraction of nanoscale metals remained inside the plants in a form compatible with the retention of at least a partial initial structure. The molecular consequences of the hyperaccumulation of nanoscale materials are discussed considering data obtained with hyperaccumulation of ionic metal. This is the first report of conventional

* Corresponding author at: Dept. Chemistry, Life Sciences and Environmental Sustainability, University of Parma, Parco Area delle Scienze 11/A, 43124 Parma, Italy.
E-mail address: nelson.marmiroli@unipr.it (N. Marmiroli).

http://dx.doi.org/10.1016/j.scitotenv.2021.152741

hyperaccumulating plants demonstrating an ability to hyperaccumulate also engineered nanomaterials (ENMs) and suggests a potential novel strategy for not only understanding plant-nanomaterial interactions but also for potential biomonitoring in the environment to avoid their entering into the food chains.

1. Introduction

Metals are important contaminants with widespread environmental distribution in soil and water (Halim et al., 2003). Although many metals are natural constituents in the Earth's crust and essential for the growth of plants and other organisms, the same elements can exert toxicity at higher concentrations. Metals (or metalloids) are considered "contaminants" when present in either a form or at a concentration that may be harmful to humans or to the environment (McIntyre, 2003). In agricultural soils, an excessive level of metals can reduce soil quality, crop yield and compromise the integrity of agricultural products, as well as cause possible hazard to humans, animals and ecosystem health.

The exploitation of plants for bioremediation of contaminated soils or "phytoremediation" has been a topic of interest for a number of years and has been attributed significant environmental and economic potential (Maestri et al., 2013; Marmiroli, 2007; Marmiroli et al., 2006; Marmiroli and McCutcheon, 2003). Approximately 400 species of plants are known as hyperaccumulators of metals as Zn, Cd, Ni, As, Co, Mn (Baker et al., 2020). By definition, the concentrations of these metals in the above ground tissues far exceeds that present in the soil: hyperaccumulation implies that metals were absorbed from the soil by the roots and translocated above to the shoot, where concentration in stem and leaves becomes quite high (Maestri et al., 2010). The level of hyperaccumulation varies with the metal, as does the resulting toxicity. For Cd, a doubling of aerial accumulation is a challenge for plants given the high toxicity of this metal. Many hyperaccumulators have been identified within the *Brassicaceae* family (Baker and Brooks, 1989), and studies have suggested an evolutionary role of hyperaccumulation as a defense against the herbivores (Behmer et al., 2005) and pests (Fones et al., 2010). *Noccaea caerulescens* (formerly *Thlaspi caerulescens*) and *Arabidopsis halleri* have been proposed as model species to study metal hyperaccumulation, (Assuncao et al., 2003) largely as a result of their genetic closeness with the model species *Arabidopsis thaliana* (L.) Heynh and because their genomes are 94% and 88.5% identical in coding regions with that of *A. thaliana*, respectively (Rigola et al., 2006).

N. caerulescens is the most extensively studied Zn and Cd hyperaccumulator: the species can accumulate these metals at concentrations exceeding 1% of shoot dry biomass. Under natural conditions, Cd seems to be less consistently hyperaccumulated than Zn (Reeves et al., 2001); the *N. caerulescens* Monte Prinzera (MP) (Italy) accession grows on serpentine soils rich in Ni and Zn and the plant hyperaccumulates both these metals. Noticeably, *N. caerulescens* is the one species currently known to hyperaccumulate Cd to over 0.01% of its shoot dry biomass (Bert et al., 2002; Reeves et al., 2001) equaled only by *N. precox* (Mišljenović et al., 2020; Zemanová et al., 2016). Pence et al. reported that in *Thlaspi caerulescens* the molecular mechanisms of Zn/Cd transport from root to shoot involved the expression of ZNT1 high-affinity transporter (Pence et al., 2000) and other authors suggest the involvement of gene NRAMP3/NRAMP4 (Oomen et al., 2009). *A. halleri* is known as hyperaccumulator of Zn but it was also found on soils with high levels of Cd; in fact, this plant can constitutively accumulate both Zn and Cd (Bert et al., 2002). *A. halleri* shares certain similarities with *N. caerulescens* in the hyperaccumulation of Zn, which is consistently observed in all natural populations. Conversely, Cd hyperaccumulation is more variable, with plants from non-metalliferous sites often showing higher degrees of metal hyperaccumulation under controlled conditions than those from metalliferous sites (Bert et al., 2002). Many hyperaccumulator species have reduced growth and metabolic rates in the absence of the metal; these plants could be at a disadvantage when resources are abundant but are favored by the high concentrations of metals in their tissues that may serve as a deterrent for animals and pests (Jiang et al., 2005; Visioli et al., 2010a).

Engineered nanomaterials (ENMs) have vast applications in superconductors, nanocrystals and solid state lighting solutions, next generation medicine, automotive components, electronics, sporting goods, environmental remediation, food, and agriculture (Caballero-Guzman and Nowack, 2016; Giese et al., 2018; Singh et al., 2021; Usman et al., 2020).

The market for quantum dots alone is projected to increase from $3 billion to $8.5 billion by 2023, with an almost 3-fold increase in production and marketing. For quantum dots, progress in nanomedicine, (Volkov, 2015) glass application for solar and nuclear power generation, glassy materials for supercapacitors and electrochemical devices are anticipated (Brow and Schmitt, 2009). Although the amount of quantum dots in the environment so far is quite low, the projected increase in production and the spread of use into areas as electronics, energy and healthcare products a significant potential as emerging contaminant (Chopra and Theis, 2017; Gottschalk et al., 2015). In addition, each boast in production will increase the likelihood for localized contamination at production sites or at specific locations during their transport. In these situations, biotechnological solutions such as phytoremediation may be a useful tool in the remediation tool box (Cota-Ruiz et al., 2018; Keller and Parker, 2019).

Soil is often the main repository for released ENMs; their small size and high surface reactivity may facilitate entry into plant cells, where both detrimental and positive effect have been noted (Hatami et al., 2016). Although some plants have shown the ability to accumulate or degrade certain nano-materials, (Cota-Ruiz et al., 2018) no species so far have been described as nanomaterial hyperaccumulator. In the present study, we showed that a Zn hyperaccumulator, *N. caerulescens*, and a Cd hyperaccumulator, *A. halleri*, also have the ability to hyperaccumulate ZnS QDs and CdS QDs, respectively. These findings open new perspectives in studying plant-nanomaterial interactions and may also be a strategy for ENM biomonitoring in the environment.

2. Methods

2.1. Hyperaccumulator and non-hyperaccumulator seed collection

Seeds of *A. halleri* Langhelsheim were kindly provided by Prof. S. Clemens (Department of Plant Physiology, University of Bayreuth, Germany); seeds of *A. thaliana* (Landsberg erecta) were obtained from the Nottingham Arabidopsis Stock Centre (NASC, University of Nottingham, United Kingdom). Seeds of *N. cearulescens* Monte Prinzera accession and of *Thlaspi perfoliatum* were taken from our collection from the Monte Prinzera site (Fornovo, Parma, Italy), a serpentine hill near Parma Italy.

2.2. Nanomaterials

The ZnS QDs and CdS QDs (uncoated) were synthesized by CNR-IMEM (Parma, Italy) following the methods of Villani et al. (2012). The CdS QDs have a bulk density of 4.82 g cm^{-3} and an average diameter of 5 nm. Cd represents 78% of the dry weight of the QD; the *Z*-potential for these nanoparticles was +61.6 mV and they have a hydrodynamic range of 1190 nm. The ZnS QDs had an average diameter under 5 nm, with Zn representing 63% of the dry weight of each QD. The ZnS QDs have a *Z*-potential of +34.9 mV and a hydrodynamic range of 248.7 nm. The purity of these products has been verified and established by TEM and X-ray diffraction spectrum. In Imperiale et al. (2022, Data in Brief) are reported method details on the determination of size, *Z*-potential and hydrodynamic range.

2.3. Soil mix preparation

Plants were grown on soil mix composed of sphagnum moss peat (33%), black peat and wood fibre (66%). The pH was 6.05 and CE was 501.3 mS/m. The soil was homogenized, sieved to 2 mm, sterilized at 120 °C and dried in an oven at 50 °C for 72 h until reaching constant weight. For this study, 300 ml plastic pots were amended with 55 g (d.w.) of soil. The metal content in the soil was determined by inductively coupled plasma-mass spectrometry (ICP-MS)(Optima 7300 DV device, Perkin Elmer, Waltham, MA, United States) and by flame atomic absorption spectrometer (FA-AAS) (AA240FS device, Agilent Technologies, California, USA), after an accurate calibration with 1000 ppm Zn standard solution and 1000 ppm Cd standard solution (Agilent Technologies, USA).

2.4. Plant growth and treatments

One seed of *N. caerulescens*, *T. perfoliatum*, *A. halleri* or *A. thaliana* was placed in each pot and was germinated in a growth chamber (MIR-554-PE, Panasonic, Osaka, Japan) for 72 h at 25 °C, under a relative humidity of 50% and dark conditions. After germination, pots with seedlings were transferred to a greenhouse with average temperatures of 25/16 °C (day/night), and light supplemented by a metal halide lamps to maintain a minimum light intensity of 300 μmol m^{-2} s^{-1}, with a 14 h photoperiod. Plants were grown for different periods prior to treatment: 45 d for *N. caerulescens* and *T. perfoliatum*, 60 d for *A. halleri* and 20 d for *A. thaliana*. The watering frequency was 30 ml of deionized water, twice a week. These conditions allowed the plants to reach approximately the same growth phase.

After the growth as above, 3 plants of each species were subjected to each treatment. *N. cearulescens* and *T. perfoliatum* exposed to 10 and 30 mg of Zn administered as $ZnSO_4$ and ZnS QDs, *A. halleri* and *A. thaliana* exposed to 10 and 30 mg of Cd administered as $CdSO_4$ and CdS QDs; three biological replicates for condition. To minimize particle aggregation, salt and NP solutions were sonicated with an Ultrasonic Cleaner USC-TH (VWR International srl, Milano, Italy) for 30 min before addition to the plants. Specifically, each plant was treated with 30 ml of a solution containing 333.33 mg L^{-1} (Cd or Zn) for the lowest concentration and 30 ml of a treatment solution containing 999.99 mg L^{-1} (Cd or Zn) for the highest concentration. The plants were then grown for an additional 30 days under the same conditions of temperature, humidity, light and irrigation. The concentrations, high and low for ion and nanoscale metals, were chosen after experiments with *A. thaliana* and *T. perfoliatum* had shown that these doses were well below those inhibiting growth.

2.5. Characterization of treatment solutions

One ml of the treatment solutions ($CdSO_4$, $ZnSO_4$) or suspensions (CdS QDs and ZnS QDs) after sonication for 30 min at 35 kHz (Transsonic T460, Elma Schmidbauer GmbH, Singen, Germany) was digested in 5 ml of 65% HNO_3 for 20 min at 165 °C with a VELP DK20 digester. After this initial digestion step, 1 ml of 30% H_2O_2 was added. The resulting solution was diluted to a final concentration of 30% HNO_3 with distilled water and the metal content was determined using FA-AAS. The solutions of QDs were analysed to determine free ions, released from the nanomaterial during the course of the experiment (Kittler et al., 2010). To do this the solutions were ultracentrifuged at 80,000 rpm for 20 min (Optima MAX-TL, Beckman Coulter, Fullerton, CA, USA) and the supernatant was analysed for metal content by ICP-MS and FA-AAS as described below.

2.6. Sampling

After 20–60 days of growth, the plants were harvested and the leaves were separated from roots, rinsed with deionized water, and weighed. Roots were thoroughly washed with deionized water to remove soil particles, weighed, and the length was measured. Each tissue sample was dried for 72 h at 70 °C, ground and homogenized. Soil samples from starting soil mix and from each treatment were collected and sieved at 2 mm.

2.7. Metal content analysis

Fifty mg of each dried sample, soil or plant, were digested in 10 ml of 65% HNO_3 (Carlo Erba, Milano, Italy) for 20 min at 165 °C and for 40 min at 230 °C with a VELP DK20 digester (Velp Scientifica S.r.l., Milano, Italy). After each digestion step, 1 ml of 30% H_2O_2 was added. The digest was filtered through a 0.45 μm mesh (Sarstead, Numbrecht, Germany) and diluted to a final concentration of 30% HNO_3 with deionized water. The Zn content in soil, roots and leaves for the *N. cearulescens* and *T. perfoliatum* experiment and Cd content in soil, roots and leaves for the *A. halleri* and *A. thaliana* experiment were determined by FA-AAS or by ICP-MS. A protocol for a more selective extraction of the ionic forms of Zn and Cd but which left substantially unaltered the nano forms of Cd and Zn or their bioconversion derivatives was developed by using milder condition as described below.

2.8. Environmental Scanning Electron Microscopy (ESEM) and X-ray microanalysis

Leaves with petioles were collected from each treatment and thoroughly washed in deionized water. Cross serial sections of petioles were prepared using carbon steel lancets (Incofar, Modena, Italy). Fresh tissue slices were positioned on 2 cm diameter stainless-steel stubs covered with double-adhesive conductive carbon tape and samples were observed with a scanning electron microscope ESEM FEG2500 FEI (FEI Europe, Eindhoven, Netherlands) operating in low-vacuum (70 Pa). For each plant, three sections of leaves and three cross sections of petioles were analysed. Details of the microscope, as well as the EDX operating parameters and data analysis are given in Imperiale et al. (2022, Data in Brief).

2.9. BCF and TF

The Bioconcentration Factor (BCF) was calculated following Zayed et al. (1998), based on the ratio between the Cd or Zn concentration found in the plant tissues to that present in the soil. The Translocation Factor (TF) was calculated as the ratio between the amount of Cd or Zn present in the aerial parts of the plant to that present in the roots. Empirical procedures used to calculate these parameters are described in Imperiale et al. (2022, Data in Brief).

2.10. Analytical evaluation of metal extractable from plant tissues after growth in different conditions

In addition to the canonical extraction procedure (65% HNO_3 for 20 min at 165 °C and 40 min at 230 °C) two mild digestion protocols were tested for the ability to extract Cd and Zn from tissues without disrupting nanoparticles. Each treatment condition was preceded by sonication for 15 min at 35 kHz (Transsonic T460, Elma Schmidbauer GmbH, Singen, Germany). First, H_2O treatment in a volume of 10 ml for 90 min was used. The solubilized metals were separated from an insoluble fraction (including the nanoparticles) by ultracentrifugation at 80,000 rpm for 20 min (Optima MAX-TL, Beckman Coulter, Fullerton, CA, USA) before their analysis with ICP-MS and FA-AAS. With a second procedure, dried plant tissues were reduced to a fine powder, kept in the muffle at 450 °C for 8 h, digested with 5% HNO_3, sonicated for 15 min at 35 kHz, ultracentrifugated as above and the supernatant was analysed for free Cd or Zn released in the supernatant. Portions of the samples remaining at the bottom were analysed by TEM-EDX to detect residual nanoparticles. Details of procedures are given in Imperiale et al. (2022, Data in Brief). A procedure for differential extraction of ionic Cd and Zn from salts and nanoscale metals was developed as described in Imperiale et al. (2022, Data in Brief). The resulting supernatant after the treatment (5% HNO_3 and H_2O) was centrifuged and then re-extracted with 65% HNO_3 at 165 °C. To confirm the specificity for ionic metal of the mild extraction procedures, the plant materials were dried and prior to extraction were spiked with concentrations (the same) of ionic and nanoscale

metals. The methods and the results are shown in Imperiale et al. (2022, Data in Brief).

2.11. Statistical analysis

Statistical significance between samples were identified by applying an ANOVA multivariate analysis, with the Tukey post-hoc test. The software package SPSS v24 (IBM website, www.ibm.com/software/it/analytics/spss/downloads.html) was used for all statistical analysis.

3. Results

3.1. Treatments of plants with Cd and Zn

The properties of the ZnS QDs and CdS QDs are shown in Fig. 2 in Imperiale et al. (2022, Data in Brief). Both particles had an average size <5 nm but they did differ substantially in z-potential, hydrodynamic range and metal content. Some properties of the plant species are shown in Fig. 3 in Imperiale et al. (2022, Data in Brief), including genetic relatedness (calculated with SSRs molecular markers) between the hyperaccumulators and non-hyperaccumulators along with their provenance.

3.2. Zn and Cd in the treatment suspensions and solutions

The measured Zn in ZnS QDs treatment suspension and in $ZnSO_4$ solution was close to the expected theoretical concentration of 333.33 mg L^{-1}; the measured values were 318.30 mg L^{-1} of Zn in ZnS QDs and 324 mg L^{-1} of Zn in $ZnSO_4$. For the higher concentration, the theoretic value was 999.99 mg L^{-1} and the measured values were 980.90 mg L^{-1} of Zn in ZnS QDs and 990.77 mg L^{-1} of Zn in $ZnSO_4$. Similarly, the concentration of Cd in the CdS QDs suspension and $CdSO_4$ solution was close to the expected theoretical of 333.33 mg L^{-1}; the measured values were 340.03 mg L^{-1} for Cd in the CdS QDs and 330.43 mg L^{-1} of Cd for $CdSO_4$. For the higher concentration of 999.99 mg L^{-1}, the measured values were 979.28 mg L^{-1} of Cd in CdS QDs and of 981.37 mg L^{-1} of Cd in the $CdSO_4$ solution.

The amount of free metal (Zn and Cd) in the NPs solutions and in the growth medium is shown in Fig. S4. For the ZnS QDs treatment, the 318.30 mg L^{-1} suspension contained 6.07 mg L^{-1} of free Zn, which represents the 1.82% on the total amount. For the CdS QDs treatment, the 340.03 mg L^{-1} suspension contained 4.06 mg L^{-1} of free Cd, which represents the 1.22% on the total Cd. Interestingly, these values were slightly modified by the presence of plant roots in the solution. The experiment was included because data in literature indicate that root exudates can increase the degradation or the transformation of a wide range of molecules and xenobiotics (Huang et al., 2017).

3.3. Zn and Cd in the soil of N. caerulescens and T. perfoliatum, A. halleri and A. thaliana

Zinc is a naturally occurring element natively present in soil, including those used for the current experiments. The initial values were 154.3 mg kg^{-1} of Zn or a total of 7.72 mg of Zn per pot. The amounts of Zn and Cd present in soil at the beginning and at the end of experiment for all the treatments is shown in Fig. 5 in Imperiale et al. (2022, Data in Brief). Cadmium was not detectable in the soil prior to treatment or at the end of experiment with the untreated soil.

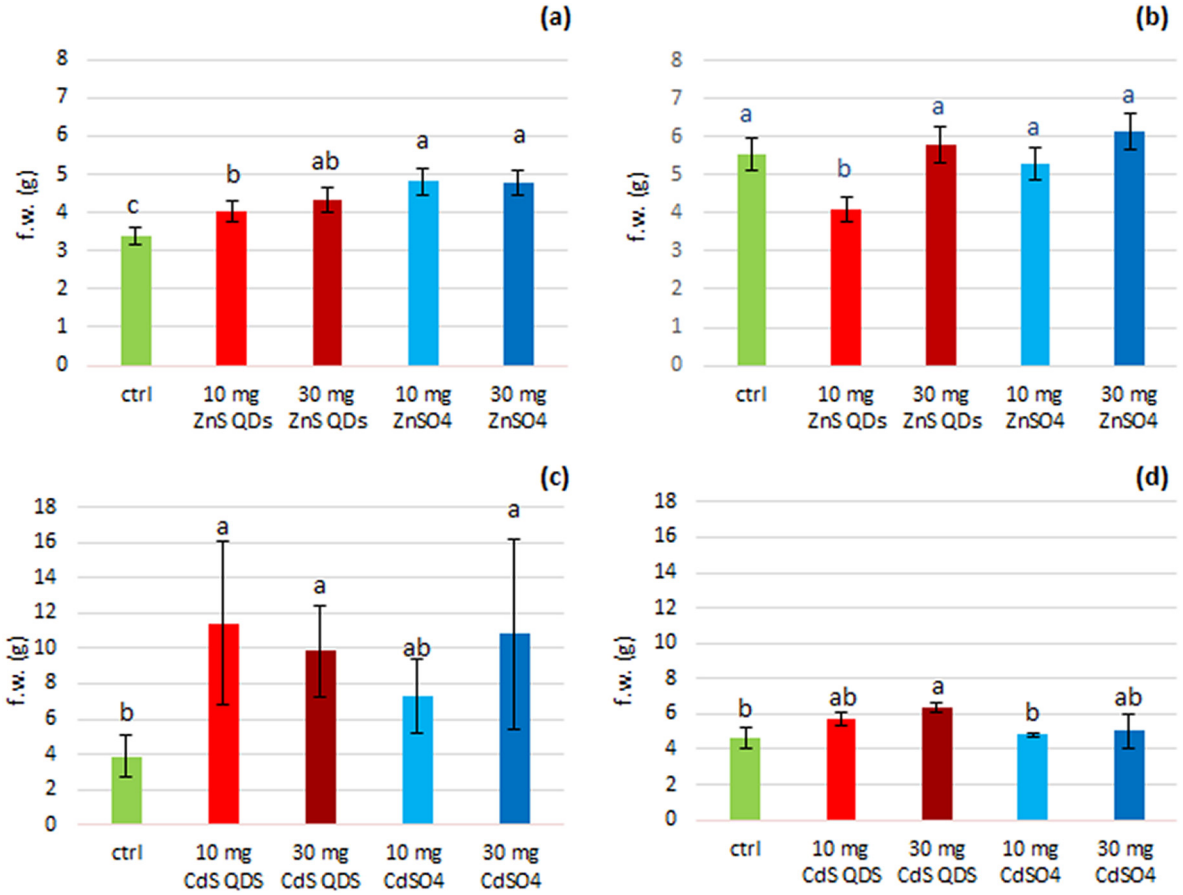

Fig. 1. Fresh weights (f.w.) of aerial tissues of *N. caerulescens* (a) and *T. perfoliatum* (b) after 30 days of treatment with Zn; *A. halleri* (c) and *A. thaliana* (d) after 30 days of treatment with Cd. Different letters indicate significant differences between means in each graph at $P < 0.05$ (ANOVA and Tukey HSD post-hoc test). The root fresh weight was excluded from the calculations.

3.4. Phenotypic variation after treatments

Some trends in phenotypic and morphological effects of treatment were evident and are shown in Fig. 1 in Imperiale et al. (2022, Data in Brief). *N. caerulescens* treated with either ZnS QDs or $ZnSO_4$ (10 and 30 mg per pot) did not show any negative symptoms on the leaf development and color. Similarly, in *T. perfoliatum* the same treatments did not produce any particular differences on plant growth and leaf morphology. However, treatment with Cd as CdS QDs at both doses (10 and 30 mg per pot) had a positive effect on growth of *A. halleri* as compared with the untreated control. Treatment with $CdSO_4$ at the lower and higher dose also had a positive effect. In *A. thaliana*, the two treatments did not produce overt phenotypic differences in growth and leaf color as compared to an untreated control (Fig. 1 in Imperiale et al. (2022, Data in Brief)).

3.5. Plants upper biomass and root length

In *N. caerulescens*, the addition of ZnS QDs and $ZnSO_4$ seemed to increase the fresh biomass of the aerial tissues. The biomass of the untreated controls weighted 3.4 g; plants treated with ZnS QDs at the low and high concentrations weighted 4.0 and 4.3 g, respectively, and plants treated with $ZnSO_4$ were 4.8 g for both treatment levels (Fig. 1); the increases are statistically significant (Fig. 1a). For *T. perfoliatum*, the addition of ZnS QDs and $ZnSO_4$ did not have a statistically significant effect on the plant biomass. The fresh mass of the aerial tissues in the untreated plants was 5.5 g; plants treated with low and high concentrations of ZnS QDs weighted 4.1 and 5.8 g, respectively, and plants treated with $ZnSO_4$ were 5.3 and 6.1 g for the lower and the higher treatment, respectively (Fig. 1b). For *A. halleri*, the addition of CdS QDs and $CdSO_4$ increased the plant biomass. The aerial tissue fresh weight for the untreated plants was 3.9 g; plants treated with high and low concentrations of CdS QDs were 11.4 and 9.8 g, respectively, and plants treated with the low and high concentrations of $CdSO_4$ were 7.3 and 10.8 g, respectively. *A. halleri*, similar to the other hyperaccumulator *N. caerulescens*, seems to benefit from exposure to Zn and Cd in both ionic and nanoscale forms; these values are statistically significant (Fig. 1c). For *A. thaliana*, the addition of CdS QDs and $CdSO_4$ did not show a significant effect on aerial tissue biomass as compared to controls. The fresh biomass of the aerial part in untreated plants was 4.6 g; plants treated with low and high concentrations of CdS QDs weighted 5.7 and 6.4 g, respectively, and plants treated with low and high concentrations of $CdSO_4$ were 4.8 and 5.0 g, respectively, with significant variation (Fig. 1d). The various treatments of ZnS QDs and $ZnSO_4$ had little impact on the root length of *N. caerulescens*, although some reduction was evident at the highest dose (30 mg) (Fig. 6a in Imperiale et al. (2022, Data in Brief)). In *T. perfoliatum*, both ZnS QDs and $ZnSO_4$ increased root length (Fig. 6b in Imperiale et al. (2022, Data in Brief)). Similarly, treatment with CdS QDs and $CdSO_4$ stimulated root growth in *A. helleri* (Fig. 6c in Imperiale et al. (2022, Data in Brief)). The root length of *A. thaliana* was differently affected by treatments (Fig. 6 in Imperiale et al. (2022, Data in Brief)). Notable, the majority of these differences were not statistically significant as compared to the untreated controls.

3.6. Zn and Cd uptake and tissue bioconcentration factor (BCF)

The amount of Zn in the root tissues of untreated plants and in plants treated with ZnS QDs and $ZnSO_4$ is shown in Fig. 2. For ZnS QDs treatments, Zn was more abundant in the roots of *N. caerulescens* (Fig. 2a) relatively to *T. perfoliatum* (Fig. 2b), whereas for $ZnSO_4$ the opposite was true. In *N. caerulescens* the addition of 30 mg of $ZnSO_4$ only, significantly increased the uptake (Fig. 2a); in *T. perfoliatum* both treatments, 10 and 30 mg of

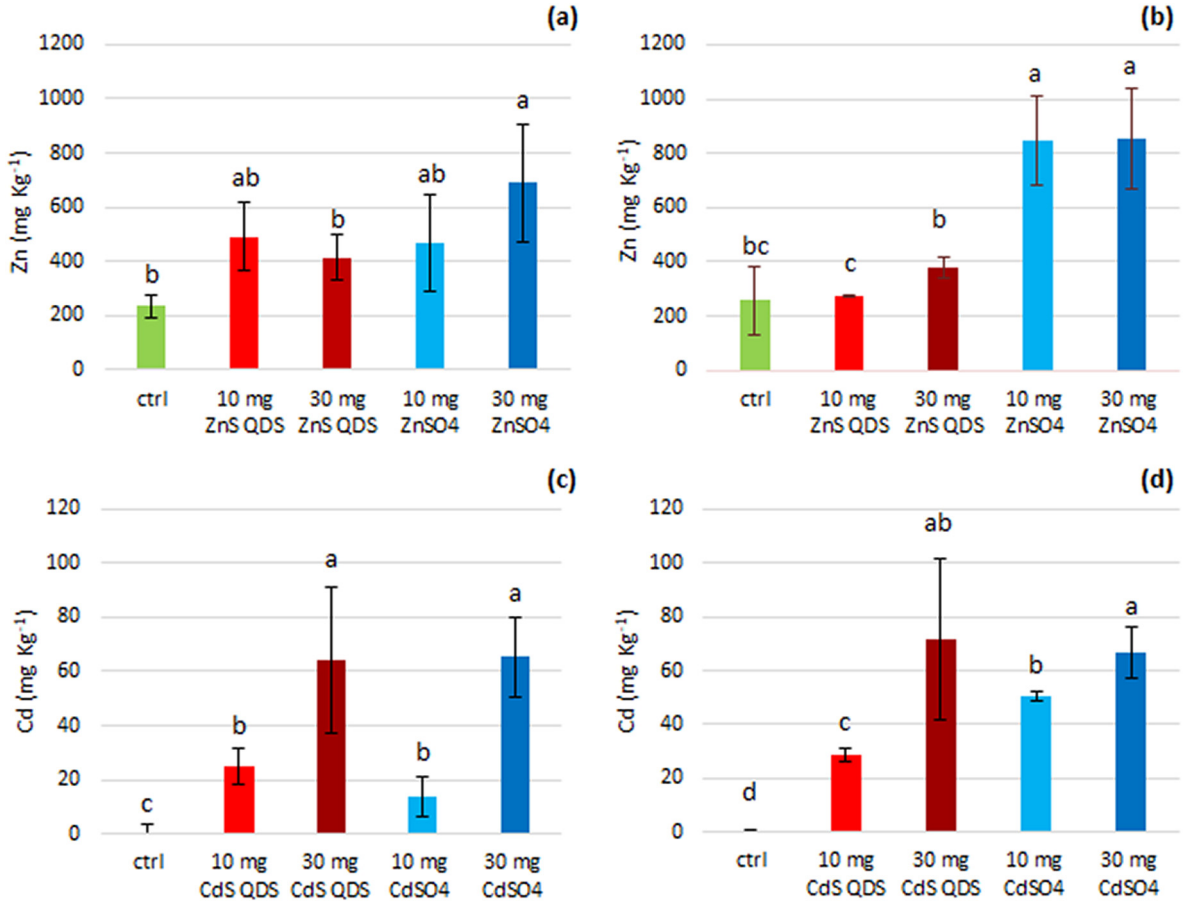

Fig. 2. Zn concentration (mg kg^{-1}) in the roots of *N. caerulescens* (a) and *T. perfoliatum* (b) after 30 days of treatment with Zn and in roots of *A. halleri* (c) and *A. thaliana* (c) after 30 days of treatment with Cd. Different letters indicate significant differences between means in each graph at $P < 0.05$ (ANOVA and Tukey HSD post-hoc test).

$ZnSO_4$, gave significant increase in Zn content as compared with control (Fig. 2b). BCF ratios were calculated for *N. caerulescens/T. perfoliatum* and for *A. halleri/A. thaliana*. Root BCFs are shown in Table 1 in Imperiale et al. (2022, Data in Brief) and Fig. 3; Fig. 3b shows the root BCF ratio between *N. caerulescens* and *T. perfoliatum*. Under ZnS QDs exposure, the ratios between BCF (roots) were >1, whereas for Zn SO_4 were <1. Untreated plants of *A. halleri* and *A. thaliana* had no detectable Cd uptake in the roots (Fig. 2c) because there was almost no Cd in the growth medium (Fig. 5 in Imperiale et al. (2022, Data in Brief)). The amount of Cd in the roots of plants treated with CdS QDs and $CdSO_4$ are shown in Fig. 2 at the begin and at the end of the growth. The amount of Cd in the roots of *A. halleri* treated with 10 and 30 mg of CdS QDs and $CdSO_4$ was statistically greater than the controls (Fig. 2c) and is comparable with that in *A. thaliana* (Fig. 3d). BCFs in the roots were also similar for the two species (Table 1 in Imperiale et al. (2022, Data in Brief)) with the exception of $CdSO_4$ (10 mg). The same is also for the root BCF ratio between *A. halleri* and *A. thaliana*. The ratios for treatments were <1 with the exception of $CdSO_4$ which was ≈1 (Fig. 3d).

For the aerial tissues of *N. caerulescens* and *T. perfoliatum*, the amount of Zn in control plants and in plants treated with ZnS QDs and $ZnSO_4$ are shown in Fig. 4a and b. Here, the differences between the two plant species are clearly evident. Across all treatments, Zn was more abundant in the aerial tissues of the hyperaccumulator *N. caerulescens* than in those of the non-hyperaccumulator *T. perfoliatum*. The BCFs in aerial tissues are shown in Table 1 in Imperiale et al. (2022, Data in Brief); Fig. 3a shows the shoot BCF ratio between the two kind of plants: 49.6 (10 mg ZnS QDs), 31.6 (30 mg ZnS QDs) and 45.9 (10 mg $ZnSO_4$), 33.7 (30 mg $ZnSO_4$). This ratio was at its maximum for the controls. Similar to the roots, the untreated plants of *A. halleri* and *A. thaliana* did not show any Cd in the shoot tissues. The concentrations of Cd in plants treated with CdS QDs and $CdSO_4$ are shown in Fig. 4c and d. In all cases, Cd was statistically more abundant in the aerial tissues of the hyperaccumulator *A. halleri* than those of the non-hyperaccumulator *A. thaliana*. Fig. 3c shows the BCF ratio of the two kind of plants treated with CdS QDs and $CdSO_4$: 2.51 (10 mg CdS QDs), 1.82 (30 mg CdS QDs) and 2.64 (10 mg $CdSO_4$), 2.22 (30 mg $CdSO_4$) (Table 1 in Imperiale et al. (2022, Data in Brief)). The differences in BCF are statistically significant from the control; with 10 mg the BCFs were similar for $CdSO_4$ and CdS QDs treatments, with 30 mg the BCF was higher for the treatment with $CdSO_4$.

3.7. Translocation factor (TF)

The calculation of TF is shown in Imperiale et al. (2022, Data in Brief) and considers transfer of the metal from the roots to the shoots. TF values are significantly higher when the hyperaccumulator is compared to the non-hyperaccumulator (Table 1 in Imperiale et al. (2022, Data in Brief)). Fig. 5 shows the TF ratios between the hyperaccumulators *N.caerulescens* and *A.halleri* with the non-hyperaccumulators *T.perfoliatum* and *A.thaliana*: for all treatments, the TF ratios are significantly higher. The TF values for ZnS QDs treatments 10 and 30 mg were 486.6 and 536.3 in *N. caerulescens* and 17.8 and 18.4 in *T.perfoliatum*, respectively. The TF values for $ZnSO_4$ treatments 10 and 30 mg were 689.9 and 378.7 in *N.caerulescens* and 8.3 and 9.1 in *T. perfoliatum*, respectively (Table S1). Calculating the ratios between TF in Zn hyperaccumulator and non-hyperaccumulator (Fig. 5a), these ratios were 27.3 and 29.1 for the treatment with 10 and 30 ZnS QDs and 82.6 and 41.6 for the treatment with 10 and 30 $ZnSO_4$, respectively.

The TF values for CdS QDs treatments 10 and 30 mg were 279.6 and 140.5 in *A. halleri* and 96.5 and 68.7 in *A. thaliana*, respectively. The TF values for $CdSO_4$ treatments 10 and 30 mg were 622.3 and 234.6 in *A. halleri* and 63.0 and 103.3 in *A. thaliana*, respectively (Table S1). The TF ratios between Cd hyperaccumulator and non-hyperaccumulator (Fig. 5b) shows a value of 2.9 and 2.0 for the treatments with 10 and 30

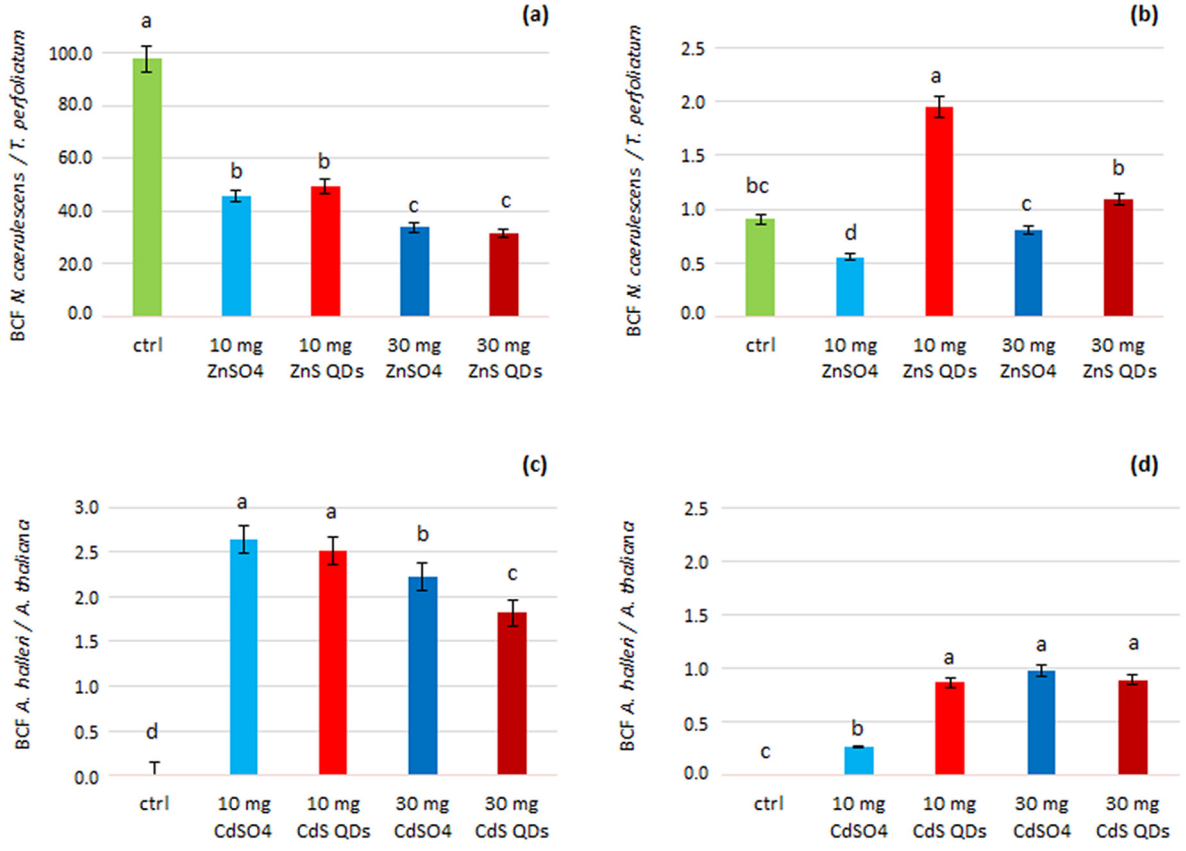

Fig. 3. Bioconcentration factor ratio (BCF-ratio) for the aerial tissues (a) and for roots (b) between *N. caerulescens* and *T. perfoliatum* after 30 days of treatment with Zn and for the aerial tissues (c) and roots (d) between *A. halleri* and *A. thaliana* after 30 days of treatment with Cd. Different letters indicate significant differences between means in each graph at $P < 0.05$ (ANOVA and Tukey HSD post-hoc test).

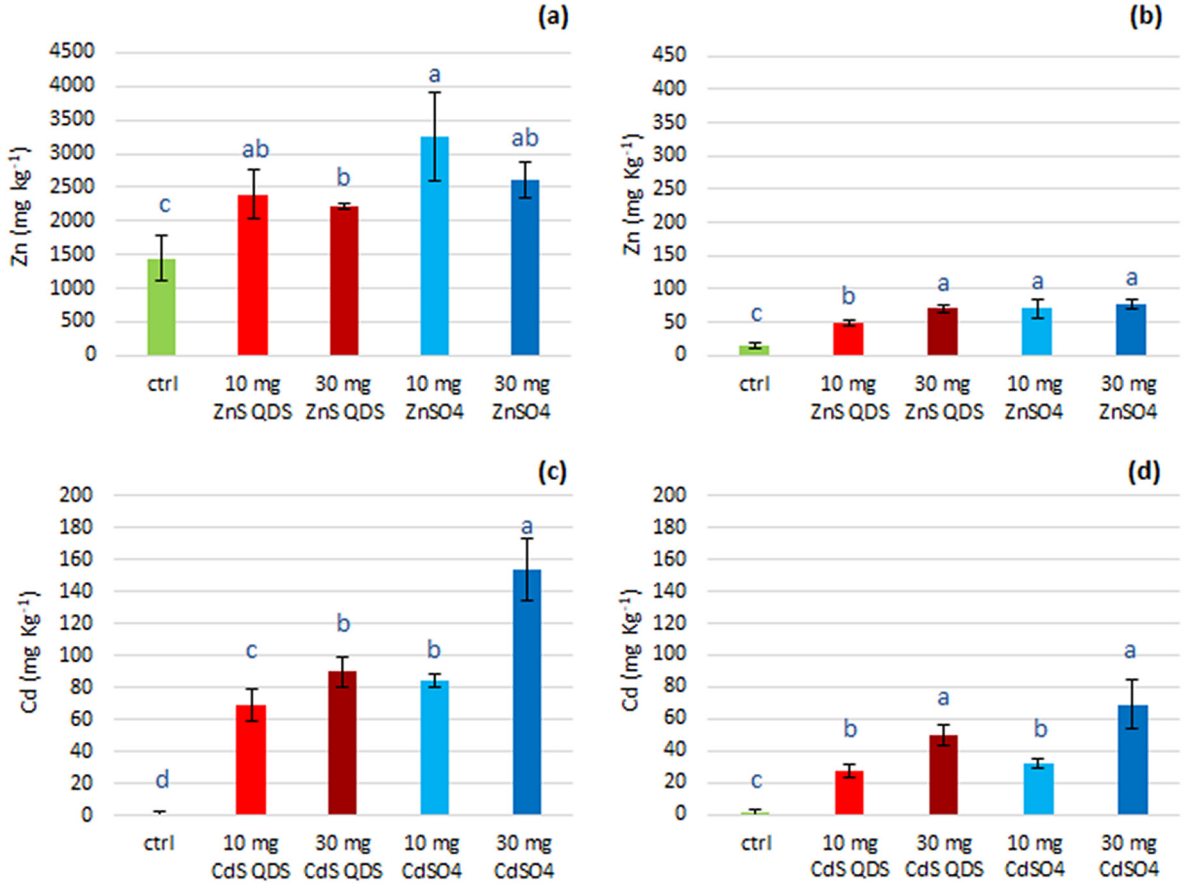

Fig. 4. Zn concentrations (mg kg^{-1}) in aerial tissues of *N. caerulescens* (a) and *T. perfoliatum* (b) after 30 days of treatment with Zn and in aerial tissues of *A. halleri* (c) and *A. thaliana* (d) after 30 days of treatment with Cd. Different letters indicate significant differences between means in each graph at $P < 0.05$ (ANOVA and Tukey HSD post-hoc test).

CdS QDs and 9.9 and 2.3 for the treatments with 10 and 30 $CdSO_4$, respectively.

3.8. ESEM analysis and X-ray imaging

N. caerulescens leaf surfaces showed no overt symptoms of phytotoxicity under any of the treatments. Under ZnS QDs exposure, the stomata were clearly visible and abundant; with $ZnSO_4$ treatment, there was a visible layer of wax on the leaf upper page, but no signs of toxicity. For both treatments, Zn Lα lines were detected in the leaf. The structure of the petioles did not vary significantly for the two types of Zn treatment; however, the amount of Zn detected within the vascular bundles was lower with ZnS QDs treatment than with $ZnSO_4$ (Fig. 6) as also shown by the AAS/ICP-MS analysis on the aerial parts of the plant. The upper leaf surfaces of *T. perfoliatum* were covered with a thick layer of waxy substances under both treatments, and this condition reduced the detection capacity of the emitted X-rays. The abundance of wax on the leaf surface can be interpreted as a stress response to the presence of Zn. Zinc was detected in leaves of the plants treated with ZnS QDs, but not with $ZnSO_4$. Under both treatments, the vascular bundles of the petioles showed traces of Zn. The leaf upper page in the exposed *A. halleri* under both treatments ($CdSO_4$ and CdS QDs) were healthy and without wax. For both treatments, the Cd Lα line was detected on the leaf surface and within the petioles vascular bundles (Fig. 6) confirm the capacity of *A. halleri* to efficiently translocate high levels of Cd. Comparing the data here with those of *A. thaliana* already published by our group, the differences are clear and striking in fact CdS QDs impact *A. thaliana* physiology and morphology (Marmiroli et al., 2019).

3.9. Chemical analysis of Zn and Cd extractable from plant tissues

Nanoscale forms of Zn and Cd are somewhat resistant to mild digestion conditions such as 5% HNO_3 and H_2O for 90 min (Fig. 7 in Imperiale et al. (2022, Data in Brief)). After mild digestion and ultracentrifugation at 80,000 rpm for 20 min, we observed that approximately 98% of the initial added metal in QD form remains insoluble at the bottom of the centrifuge tube. Conversely, when Cd or Zn salts are subjected to similar mild digestion protocols, nearly all of Cd and Zn were detectable in solution. The difference between salt and nanoforms became even more striking when the solubilisation was done with H_2O with a small addition of 30% H_2O_2. Consequently, these procedures were compared to determining the amounts of metals extractable from plant tissues after treatments with Zn and Cd as salts or in nanoscale form (Fig. 7 in Imperiale et al. (2022, Data in Brief)). Specifically, three digestions conditions were compared: 1) 65% HNO_3 for 20 min at 165 °C and for 40 min at 230 °C, as well as the two mild treatments 2) 5% HNO_3 and 3) H_2O for both 90 min at room temperature with small addition of 30% H_2O_2. The supernatant of control samples, which were not added with any ZnS QDs, indeed contained a certain amount of Zn (about 50% of total Zn) under both mild treatments due to the Zn present in the growth medium and the procedure was considerably less effective than total digestion with 65% HNO_3 at 165 °C and 230 °C. From this test we can assume that about 50% of the total Zn, in the samples grown with nanoscale Zn, is in a relatively insoluble form. In the samples treated with $ZnSO_4$, the amount of Zn extracted with 5% HNO_3 was only 41%. In the samples treated with ZnS QDs, the freely extractable Zn by mild HNO_3 digestion was about 50%. Notably, the amount of insoluble metal after treatment remained about 50–55% in all three Zn amendment scenarios: non-treated, ZnS QDs and with $ZnSO_4$. These findings may fit with

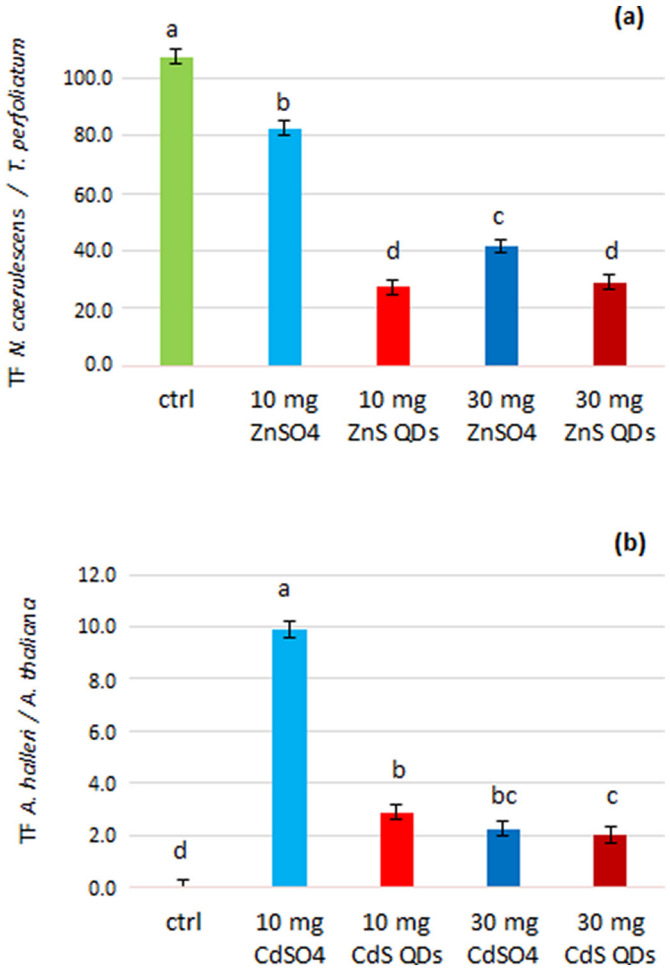

Fig. 5. Translocation factor ratio (TF ratio) of *N. caerulescens* and *T. perfoliatum* after 30 days of treatment with Zn (a) and of *A. halleri* and *A. thaliana* after 30 days of treatment with Cd (b). Different letters indicate significant differences between means in each graph at $P < 0.05$ (ANOVA and Tukey HSD post-hoc test).

observations that metals may exist within the tissues in complex forms with metal-S and metal-O bounds as previously suggested (Callahan et al., 2006). These findings were recently confirmed in Arabidopsis exposed to CdS QDs (Marmiroli et al., 2020). In an additional test, the plant tissue was converted to a fine powder by heating at 450 °C for 7.5 h (Fig. 7). This should allow to a concentration of any elements including Zn. The dehydrated powder was than treated with 5% HNO_3 and the suspension was ultracentrifuged before more rigorous digestion of supernatant with 65% HNO_3. The total amounts of Zn extractable from the ash of control and Zn QDs treated samples were approximately the same due to the high Zn in growth medium. It was higher when $ZnSO_4$ was added to the plant (Fig. 7a). However, the ratio of Zn in the untreated samples to that of samples treated with $ZnSO_4$ was similar (0.87 and 0.83), whereas that of samples treated with Zn QDs was lower (0.57) (Fig. 7b). These findings indicate that were less extractable Zn in condition of treatment with ZnS QDs, although the total amount of Zn in tissues was about the same (Fig. 7). The procedure of hard-drying performed on the three samples highlights a greater stability of Zn when added in the form of QDs as compared with Zn salt. To confirm the reliability of the analytical approach a reconstruction experiment was performed. Another experiment of differential digestion was conducted as indicated in Fig. 8 in Imperiale et al. (2022, Data in Brief). In this experiment the dried powders of tissues were supplemented with 10 mg of Zn salt or nanoscale Zn and then treated as indicated. After the extraction with 65% HNO_3, 5% HNO_3, H_2O the samples were centrifuged and each supernatants furtherly extracted with 65% HNO_3. The results also in this case showed that the treatments yielded a differential extraction of ionic and nano Zn with the mild procedures and in particular, with H_2O amended with 30% H_2O_2. Only 1/7 of the Zn extractable from the sample added with $ZnSO_4$ was extractable when the sample was supplemented with ZnS QDs. On the other hand, the Zn extractable from the same type of treatment when the digestion was with 65% HNO_3 at high temperature, was 2/3 of the value obtained in the sample added with $ZnSO_4$. In the samples added with $ZnSO_4$ and the extraction performed with 5% HNO_3 this ratio became 1/2 (Table S2). If the supernatants were not subjected to the last digestion with 65% HNO_3, the values obtained with the two mild digestion procedures were those reported in Table S3. In particular in the extraction with 5% HNO_3 the Zn released from the sample added with ZnS QDs was 50% of that supplemented with $ZnSO_4$, and in the extraction with H_2O the Zn released from the sample added with ZnS QDs was less than 1% of that supplemented with $ZnSO_4$. In these cases after ultracentrifugation of samples added with comes from nanoscale Zn and to mild digestion, the SEM-EDX analysis of the pellets showed the presence of nanoparticles (data not shown).

3.10. TEM-EDX analysis of dehydrated plant tissues

The dehydrated ashes from plants of *N. caerulescens* treated with ZnS QDs or *A. halleri* treated with CdS QDs were therefore thoroughly washed with H_2O, filtered and rehydrated and then analysed by TEM-EDX. EDX imaging indicated a large distribution of both Zn and Cd amongst the fine particles of the ashes; the distribution of the metals partially overlapped with that of S (Fig. 9 in Imperiale et al. (2022, Data in Brief)). It is convincible that this indicate that a significant amount of Zn and Cd in the nanoform remained entrapped within the plant tissues after the treatment in the pristine form or bioconverted as suggested (Marmiroli et al., 2020) though a significant portion probably is converted in more water soluble forms.

4. Discussion

Engineered nanomaterial (ENMs) use has expanded in a number of sectors, including energy, electronics and agriculture (Caballero-Guzman and Nowack, 2016; Giese et al., 2018). Given that the final sink for many of these materials will be the soil, a significant amount of research has begun to focus on ENMs interactions with plant species (Cota-Ruiz et al., 2018; Pagano et al., 2018b). Many forms of ENMs have a sufficiently small size and high surface reactivity to facilitate rapid entry into cells, often with the formation of a biologically derived coating or "protein corona" that facilitate the interaction (Ruotolo et al., 2018). Once in the environment, ENMs undergo particle-specific transformation and aggregation reactions with soil organic matter and other environmental compartments (Keller et al., 2013). which can lead to increased stability or to increased solubility with subsequent ion release (Garner et al., 2017; Tan et al., 2017). As a commonly used ENM, quantum dots have metal cores of Zn and Cd such as those used in the current study (CdS QDs and ZnS QDs); These types of nanomaterials have high stability under a range of experimental/environmental conditions and often release only small quantities of ions. Upon exposure to QDs, plants can show inhibition of cell functions such as respiration and photosynthesis, often associated with decreased growth and large changes in gene transcription and protein synthesis (Gallo et al., 2020; Miralles et al., 2012; Pagano et al., 2016, 2018c).

The current study reports how the Zn and Cd translocated from roots to leaves in the hyperaccumulators *N. caerulescens* (Zn) and *A. halleri* (Cd) was quantitally similar when the source supplied to medium were salts or QDs. But, the two hyperaccumulators did not show any overt signs of toxicity,

Fig. 6. Above in each box: ESEM images of representative upper leaf pages and vascular bundles. Acceleration voltage 5 keV, pressure 60 Pa, working distance 10 mm, pinhole aperture 2.5 μm. White bars at bottom left indicate the magnification. Below in each box: EDX spectra of the yellow rectangle in the SEM image above: acceleration voltage 20 keV, acquisition time 60 s. Spectra are completely deconvoluted using the PB/ZAF method.

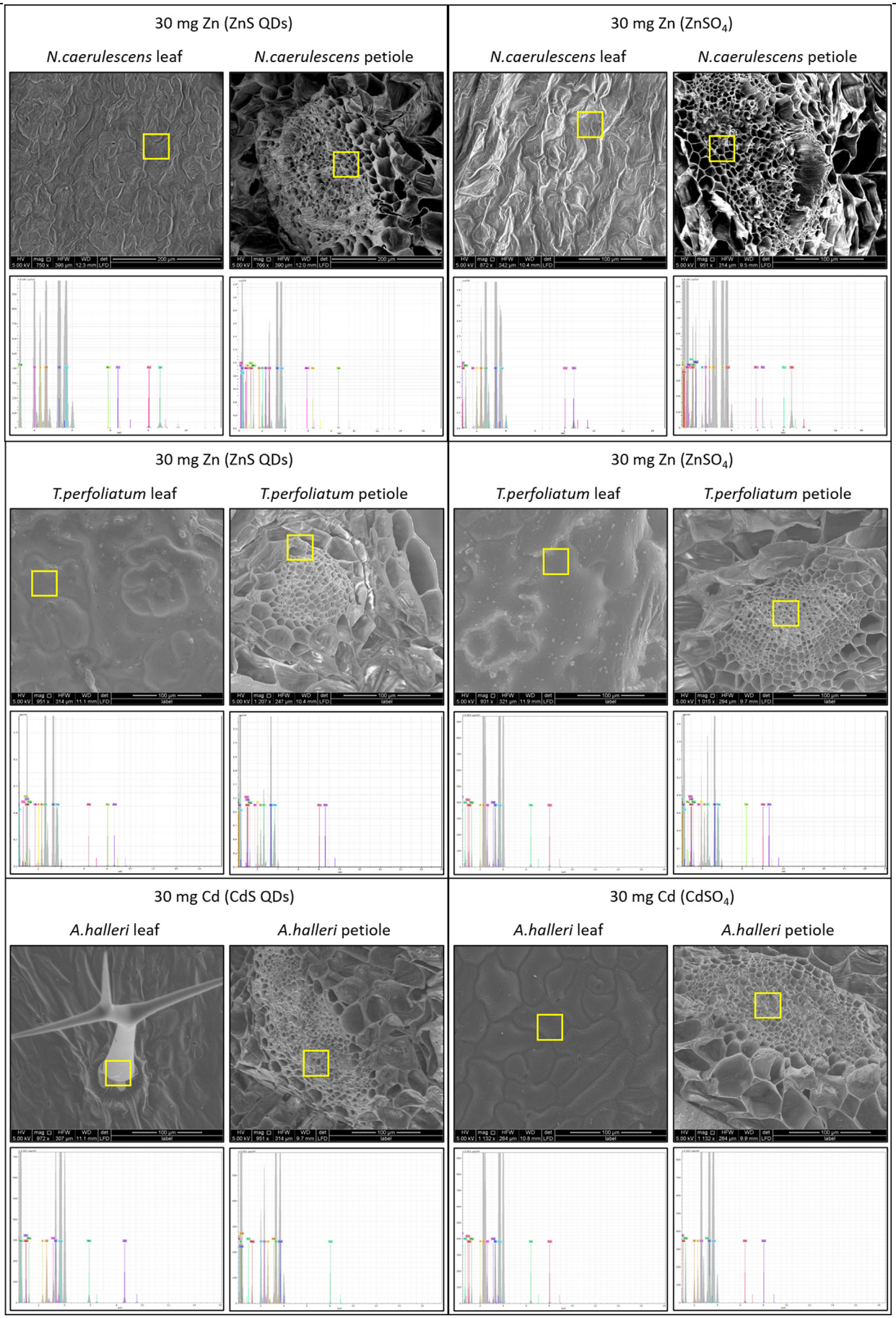
30 mg Zn (ZnS QDs)
N.caerulescens leaf
N.caerulescens petiole
30 mg Zn ($ZnSO_4$)
N.caerulescens leaf
N.caerulescens petiole
30 mg Zn (ZnS QDs)
T.perfoliatum leaf
T.perfoliatum petiole
30 mg Zn ($ZnSO_4$)
T.perfoliatum leaf
T.perfoliatum petiole
30 mg Cd (CdS QDs)
A.halleri leaf
A.halleri petiole
30 mg Cd ($CdSO_4$)
A.halleri leaf
A.halleri petiole

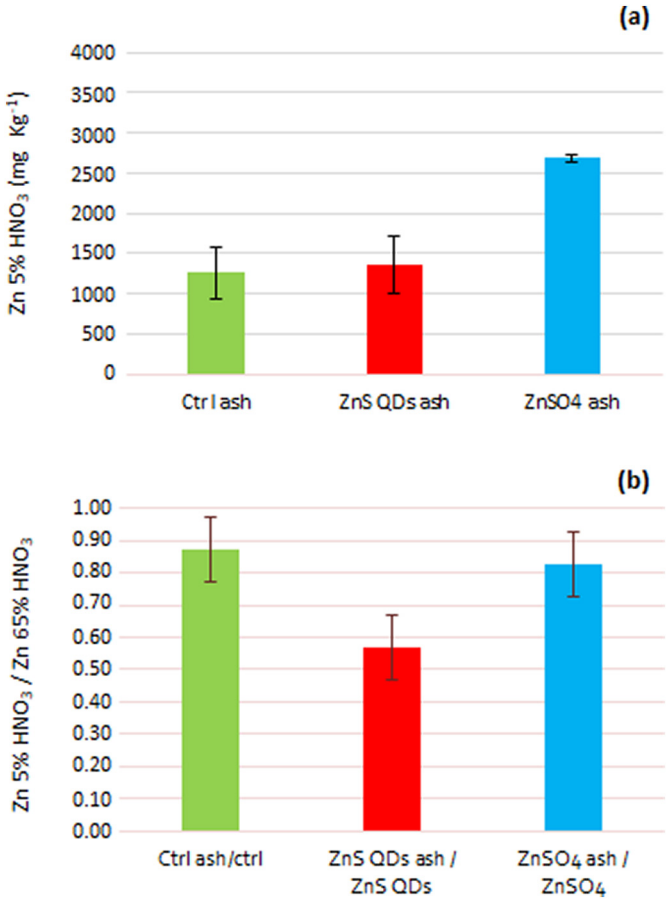

Fig. 7. Zn concentrations (mg kg^{-1}) in the tissue ash of treated *N. caerulescens* after a mild digestion with 5% HNO_3 (a) and the ratio with the Zn concentration found in the plant tissues after the same was digested with 65% HNO_3 (b).

such as reduction of root and shoot growth, when exposed to metal or nanoscale metal. The total amounts of metal ions and nanoscale metals translocated to the aerial parts of the *A. halleri* and *N. caerulescens* was significant but for Cd not as high as other reports for these species; (Marques et al., 2009) this can likely be explained by differences in experimental design and exposure (Visioli et al., 2010b) and by the fact that the presence of a certain amount of Zn in the growth medium may inhibit the uptake of Cd because it depends on the concentration of both metals in the medium. But, the three basic properties of hyperaccumulators, are maintained under these conditions. First, the shoot bioconcentration ratio (BCF ratio) and the root to shoot translocation ratio (TF ratio) were consistently greater than 1.0 (McGrath et al., 2006; McGrath and Zhao, 2003). Second, the amount of Zn in the shoots of *N. caerulescens* treated with nanoscale Zn was 0.23% of the DW; the value was 0.29% of DW for the ionic form. The amount of Cd in *A. halleri* shoots upon treatment with nanoscale Cd was 0.008% of the DW; the value for the ionic form was 0.012% of DW (Baker and Brooks, 1989). Third, the hyperaccumulator *N. caerulescens* has a BCF (for ionic form and nanoscale) for Zn that is 31.9–49.6 that of the non-hyperaccumulator *T. perfoliatum*; the *A. halleri* BCF for Cd was 1.82–2.64 that of *A. thaliana*. Importantly, plant morphology and biomass indicate greater tolerance for Zn and Cd in *N. caerulescens* and *A. helleri* then in their non-hyperaccumulators relatives.

A relatively limited number of studies have definitively shown the fate of ENMs in plant tissues. Synchrotron radiation (μXRF and μXANES) has been used to show the atomic environment of Ti after uptake and translocation of TiO_2 nanoparticles in cucumber plants (Servin et al., 2012) and more recently also the fate of CdS QDs in *A. thaliana* was shown (Marmiroli et al., 2020). The same technique was used to study uptake and translocation of Cd^{2+} and Zn^{2+} ions in *A. halleri* and *N. caerulescens* (Huguet et al., 2012; Isaure et al., 2015; Küpper et al., 2004). In the current study, analytical techniques together with microscopic (TEM-EDX and ESEM-EDX) tools were used to evaluate the interaction of ZnS QDs and CdS QDs in different plant tissues. The evidences obtained, thoroughly correlative, suggests that a significant amount of the metals were inside the plant vessels and leaves after treatment in a nanoscale or a non-ionic form. Because these analyses were made on plants exposed for 30 days, during that period the nanoscale metals can have been transformed in a less structured and not equally stable form which was not the case because the nanoscale metals maintained 30 days in the growth medium did not increase their extractability by H_2O (data not shown). It will be important in the future to understand if the nanoscale metals in the hyperaccumulators were bound by strong specific ligands within the plant cells (Krämer et al., 1996) or if they are more loosely associated with organic acids or amino acids that are abundant within the plant vacuoles (Salt et al., 1999). It has been demonstrated that in *N. caerulescens*, phytochelatins are an important metal-binding ligand that facilitate metal compartmentalization in the cells or vacuoles, effectively reducing harm to cell function by toxic metals (Ebbs et al., 2002; Psaras and Manetas, 2001).

5. Conclusions

The biological function of ENMs depends on their physicochemical properties but also on their capacity to enter into the plant (Pagano et al., 2017; Servin et al., 2017). Series of studies report that, for ENMs of larger size (>40 nm) the size of the cell wall's pore is the limiting factor in uptaking ENMs into the plant. The second conditioning factor is the nature of ENMs which can promote or inhibit the attachment to the radical surfaces or to the radical exudates (Ali et al., 2021).

For smaller ENMs as our QDs (3 to 5 nm) they do enter into the plant roots using either osmotic pressure, capillary forces or directly through the epidermal cells. Once they have crossed the cells wall, they are transported via apoplast until they reach the central vascular cylinder, ENMs need to cross the Casparian strip barrier which in normal conditions ENMs can make by crossing plasma membrane and then into the xylem (Miralles et al., 2012). When they have reached the vascular system ENMs could be translocated to the aerial part via the transpiration stream (Miralles et al., 2012). Studies with isolated cells suggest that an endocytic pathway may be involved with an active transport through vesicles from the plasma membrane which are also participants in nutrient uptake, regulation of plasma membrane receptors and in membrane recycling (Ovečka et al., 2005).

The uptake of nanoscale metals (Cd/Zn) by the two hyperaccumulator certainly benefits of this vesicular transport, but it is not consequent that the uptake was more effective than in the non-hyperaccumulator. In fact root uptakes remained quite comparable whereas significantly larger was (in the hyperaccumulators) the BFs and TFs; meaning a larger tolerance of stem and leaves to the metals in either forms (ionic or nano). Tolerance to the metals in hyperaccumulators was related to specific chelating proteins and organic acid (Małgorzata et al., 2020; Zhao et al., 2006) whereas for nanomaterial other mechanisms like biotransformation were also involved (Majumdar et al., 2019; Marmiroli et al., 2020).

But the mechanism of internalization may also involve the formation of a “corona” around ENMs constituted also of tightly bound proteins (hard corona) which can have a relevant role in the mechanism of displacement but also of phytotoxicity (Ruotolo et al., 2018). According to results so far obtained there are therefore differences between uptake and internalization of metals when in ionic or in nanoscale forms with the involvement of different transport mechanisms (De La Torre Roche et al., 2018; Małgorzata et al., 2020; Pence et al., 2000; Servin et al., 2017).

But also the mechanism of phytotoxicity seems different from ionic and nanoscale metals. This has been shown in particular for Zn and Cd and in general for different metals and non-metals (Marmiroli et al., 2014, 2019; Pagano et al., 2018a). Beyond many positive effects on plants and crop

plants (Ali et al., 2021; Gardea-Torresdey et al., 2014; Kah et al., 2019; Lowry et al., 2019) there are some risks to be considered when dispersion of ENM in the environment is concerned.

The accurate measurement of ENMs in the environment is generally low and difficult to achieve; as such, environmental risk assessment efforts largely rely on exposure modeling (Keller and Parker, 2019). Exposure estimates for QD were reported and discussed by Gottschalk et al. (2015). The possibility of reaching significant concentrations similar to that of carbon black and TiO_2 is possible given the increased production and use of some types of quantum dots including ZnS QDs and CdS QDs. Given their specific uses, future contamination in the environment will likely be heterogeneous (Chopra and Theis, 2017; Zuverza-Mena and White, 2018). The application to healthcare and to new energy systems could lead to a concentration in wastes, wastewaters and sludges associated with the sites of production. In particular, quantum dots used in nanomedicine could lead to a particularly difficult emerging environmental challenge (Baun and Hansen, 2008; Gardea-Torresdey et al., 2014). Data for relevant ecotoxicological end points is a knowledge gap that must be addressed. The discovery that two plant species such as *N. caerulescens* and *A. halleri* may also hyperaccumulate Zn and Cd also in the nanoscale forms certainly is evidence of a new hazard that should trigger additional research on both the mechanisms of accumulation and also on understanding the subsequent risk for environmental and human health. The fact that *A. halleri* and *N. caerulescens* grow slowly and produce relatively low biomass (McGrath and Zhao, 2003) precludes their use for phytoextraction of these novel contaminants. However, these species may serve to an effective environmental biomonitoring.

CRediT authorship contribution statement

Davide Imperiale: Data curation, Formal analysis, Investigation, Writing – original draft. **Giacomo Lencioni:** Formal analysis, Investigation. **Marta Marmiroli:** Formal analysis, Investigation, Writing – review & editing. **Andrea Zappettini:** Validation, Writing – review & editing. **Jason C. White:** Validation, Writing – review & editing. **Nelson Marmiroli:** Conceptualization, Funding acquisition, Supervision, Writing – review & editing.

Declaration of competing interest

The authors declare that they have no known competing financial interests or personal relationships that could have appeared to influence the work reported in this paper.

Acknowledgements

The authors wish to thank “Riserva Naturale del Monte Prinzera” (Fornovo, Parma, Italy), who gave access to collection of natural materials both *N. caerulescens* and *T. perfoliatum* in different periods through which the research lasted. Thanks also to Prof. Clemens (Department of Plant Physiology, University of Bayreuth, Germany) who kindly provided the *A. halleri* plants. Thanks also Dr. M. Villani from IMEM-CNR for contributing the TEM-EDX analysis. The project was carried out thanks to the contribution of the University of Parma, CINSA and IMEM who covered part of the costs. JCW acknowledges USDA NIFA CONH00147. Preliminary results of this paper were presented at the 15th International Phytotechnology Conference in Novi Sad (Serbia) in 2018 and many of the discussions and comments were invaluable for the preparation of this article.

Appendix A. Supplementary data

Supplementary data to this article can be found online at https://doi.org/10.1016/j.scitotenv.2021.152741.

References

Ali, S., Mehmood, A., Khan, N., 2021. Uptake, translocation, and consequences of nanomaterials on plant growth and stress adaptation. J. Nanomater. 2021. https://doi.org/10.1155/2021/6677616.

Assuncao, A.G.L., Schat, H., Aarts, M.G.M., 2003. Thlaspi caerulescens, an attractive model species to study heavy metal hyperaccumulation in plants. New Phytol. 159, 351–360. https://doi.org/10.1046/j.1469-8137.2003.00820.x.

Baker and Brooks, 1989. Terrestrial higher plants which hyperaccumulate metallic elements - a review of their distribution, ecology and phytochemistry. Biorecovery 1, 81–126. https://doi.org/10.1093/toxsci/kfg183.

Baker, A.J.M., McGrath, S.P., Reeves, R.D., Smith, J.A.C., 2020. Metal hyperaccumulator plants: a review of the ecology and physiology of a biological resource for phytoremediation of metal-polluted soils. Phytoremediat. Contam. Soil Water, 85–107 https://doi.org/10.1201/9780367803148-5.

Baun, A., Hansen, S.F., 2008. Environmental challenges for nanomedicine. Nanomedicine 3, 605–608. https://doi.org/10.2217/17435889.3.5.605.

Behmer, S.T., Lloyd, C.M., Raubenheimer, D., Stewart-Clark, J., Knight, J., Leighton, R.S., Harper, F.A., Smith, J.A.C., 2005. Metal hyperaccumulation in plants: mechanisms of defence against insect herbivores. Funct. Ecol. 19, 55–66. https://doi.org/10.1111/j.0269-8463.2005.00943.x.

Bert, V., Bonnin, I., Saumitou-Laprade, P., de Laguerie, P., Petit, D., 2002. Do Arabidopsis halleri from nonmetallicolous populations accumulate zinc and cadmium more effectively than those from metallicolous populations? New Phytol. 155, 47–57. https://doi.org/10.1046/j.1469-8137.2002.00432.x.

Brow, R.K., Schmitt, M.L., 2009. A survey of energy and environmental applications of glass. J. Eur. Ceram. Soc. 29, 1193–1201. https://doi.org/10.1016/J.JEURCERAMSOC.2008.08.011.

Caballero-Guzman, A., Nowack, B., 2016. A critical review of engineered nanomaterial release data: are current data useful for material flow modeling? Environ. Pollut. 213, 502–517. https://doi.org/10.1016/J.ENVPOL.2016.02.028.

Callahan, D.L., Baker, A.J.M., Kolev, S.D., Wedd, A.G., 2006. Metal ion ligands in hyperaccumulating plants. JBIC J. Biol. Inorg. Chem. 11, 2–12. https://doi.org/10.1007/s00775-005-0056-7.

Chopra, S.S., Theis, T.L., 2017. Comparative cradle-to-gate energy assessment of indium phosphide and cadmium selenide quantum dot displays. Environ. Sci. Nano 4, 244–254. https://doi.org/10.1039/C6EN00326E.

Cota-Ruiz, K., Delgado-Rios, M., Martínez-Martínez, A., Núñez-Gastelum, J.A., Peralta-Videa, J.R., Gardea-Torresdey, J.L., 2018. Current findings on terrestrial plants – engineered nanomaterial interactions: are plants capable of phytoremediating nanomaterials from soil? Curr. Opin. Environ. Sci. Health 6, 9–15. https://doi.org/10.1016/J.COESH.2018.06.005.

Salt, David E., Prince, Roger C., Baker, Alan J.M., Pickering, I.J., Raskin, Ilya, 1999. Zinc Ligands in the Metal Hyperaccumulator Thlaspi caerulescens As Determined Using X-ray Absorption Spectroscopy.

De La Torre Roche, R., Pagano, L., Majumdar, S., Eitzer, B.D., Zuverza-Mena, N., Ma, C., Servin, A.D., Marmiroli, N., Dhankher, O.P., White, J.C., 2018. Co-exposure of imidacloprid and nanoparticle ag or CeO2 to Cucurbita pepo (zucchini): contaminant bioaccumulation and translocation. NanoImpact 11, 136–145. https://doi.org/10.1016/J.IMPACT.2018.07.001.

Ebbs, S., Ahner, B., Kochian, L., Lau, I., 2002. Phytochelatin synthesis is not responsible for Cd tolerance in the Zn/Cd hyperaccumulator Thlaspi caerulescens (J. & C. Presl). Planta 214, 635–640. https://doi.org/10.1007/s004250100650.

Fones, H., Davis, C.A.R., Rico, A., Fang, F., Smith, J.A.C., Preston, G.M., 2010. Metal hyperaccumulation armors plants against disease. PLoS Pathog. 6, e1001093. https://doi.org/10.1371/journal.ppat.1001093.

Gallo, V., Srivastava, V., Bulone, V., Zappettini, A., Villani, M., Marmiroli, N., Marmiroli, M., 2020. Proteomic analysis identifies markers of exposure to cadmium sulphide quantum dots (CdS QDs). Nanomaterials 10, 1214. https://doi.org/10.3390/nano10061214.

Gardea-Torresdey, J.L., Rico, C.M., White, J.C., 2014. Trophic transfer, transformation, and impact of engineered nanomaterials in terrestrial environments. Environ. Sci. Technol. 48, 2526–2540. https://doi.org/10.1021/es4050665.

Garner, K.L., Suh, S., Keller, A.A., 2017. Assessing the risk of engineered nanomaterials in the environment: development and application of the nanofate model. Environ. Sci. Technol. 51, 5541–5551. https://doi.org/10.1021/acs.est.6b05279.

Giese, B., Klaessig, F., Park, B., Kaegi, R., Steinfeldt, M., Wigger, H., von Gleich, A., Gottschalk, F., 2018. Risks, release and concentrations of engineered nanomaterial in the environment. Sci. Rep. 8, 1565. https://doi.org/10.1038/s41598-018-19275-4.

Gottschalk, F., Lassen, C., Kjoelholt, J., Christensen, F., Nowack, B., 2015. Modeling flows and concentrations of nine engineered nanomaterials in the danish environment. Int. J. Environ. Res. Public Health 12, 5581–5602. https://doi.org/10.3390/ijerph120505581.

Halim, M., Conte, P., Piccolo, A., 2003. Potential availability of heavy metals to phytoextraction from contaminated soils induced by exogenous humic substances. Chemosphere 52, 265–275. https://doi.org/10.1016/S0045-6535(03)00185-1.

Hatami, M., Kariman, K., Ghorbanpour, M., 2016. Engineered nanomaterial-mediated changes in the metabolism of terrestrial plants. Sci. Total Environ. 571, 275–291. https://doi.org/10.1016/J.SCITOTENV.2016.07.184.

Huang, Y., Zhao, L., Keller, A.A., 2017. Interactions, transformations, and bioavailability of nano-copper exposed to root exudates. Environ. Sci. Technol 51, 38. https://doi.org/10.1021/acs.est.7b02523.

Huguet, S., Bert, V., Laboudigue, A., Barthès, V., Isaure, M.P., Llorens, I., Schat, H., Sarret, G., 2012. Cd speciation and localization in the hyperaccumulator Arabidopsis halleri. Environ. Exp. Bot. 82, 54–65. https://doi.org/10.1016/j.envexpbot.2012.03.011.

Imperiale, D., Lencioni, G., Marmiroli, M., Zappettini, A., White, J.C., Marmiroli, N., 2022. Data on the interaction of hyperaccumulating plants with nanoscale metals Zn and Cd. Data in Brief Submitted for publication.

Isaure, M.P., Huguet, S., Meyer, C.L., Castillo-Michel, H., Testemale, D., Vantelon, D., Saumitou-Laprade, P., Verbruggen, N., Sarret, G., 2015. Evidence of various mechanisms of Cd sequestration in the hyperaccumulator Arabidopsis halleri, the non-accumulator Arabidopsis lyrata, and their progenies by combined synchrotron-based techniques. J. Exp. Bot. 66, 3201–3214. https://doi.org/10.1093/jxb/erv131.

Jiang, R.F., Ma, D.Y., Zhao, F.J., Mcgrath, S.P., 2005. Cadmium Hyperaccumulation Protects Thlaspi caerulescens From Leaf Feeding Damage by Thrips (Frankliniella occidentalis). https://doi.org/10.1111/j.1469-8137.2005.01452.x.

Kah, M., Tufenkji, N., White, J.C., 2019. Nano-enabled strategies to enhance crop nutrition and protection. Nat. Nanotechnol. https://doi.org/10.1038/s41565-019-0439-5.

Keller, A.A., McFerran, S., Lazareva, A., Suh, S., 2013. Global life cycle releases of engineered nanomaterials. J. Nanopart. Res. 15, 1692. https://doi.org/10.1007/s11051-013-1692-4.

Keller, A.A., Parker, N., 2019. Innovation in procedures for human and ecological health risk assessment of engineered nanomaterials. Expo. Eng. Nanomater. Environ. 185–208. https://doi.org/10.1016/B978-0-12-814835-8.00007-8.

Kittler, S., Greulich, C., Diendorf, J., Köller, M., Epple, M., 2010. Toxicity of silver nanoparticles increases during storage because of slow dissolution under release of silver ions. Chem. Mater. 22, 4548–4554. https://doi.org/10.1021/cm100023p.

Krämer, U., Cotter-Howells, J.D., Charnock, J.M., Baker, A.J.M., Smith, J.A.C., 1996. Free histidine as a metal chelator in plants that accumulate nickel. Nature 379, 635–638. https://doi.org/10.1038/379635a0.

Küpper, H., Mijovilovich, A., Meyer-Klaucke, W., Kroneck, P.M.H., 2004. Tissue-and age-dependent differences in the complexation of cadmium and zinc in the cadmium/zinc hyperaccumulator Thlaspi caerulescens (Ganges ecotype) revealed by X-Ray absorption spectroscopy 1[w]. Plant Physiol. 134, 748–757. https://doi.org/10.1104/pp.103.032953.

Lowry, G.V., Avellan, A., Gilbertson, L.M., 2019. Opportunities and challenges for nanotechnology in the agri-tech revolution. Nat. Nanotechnol. 14, 517–522. https://doi.org/10.1038/s41565-019-0461-7.

Maestri, E., Marmiroli, M., Visioli, G., Marmiroli, N., 2010. Metal tolerance and hyperaccumulation: costs and trade-offs between traits and environment. Environ. Exp. Bot. 68, 1–13. https://doi.org/10.1016/J.ENVEXPBOT.2009.10.011.

Maestri, E., Pirondini, A., Visioli, G., Marmiroli, N., 2013. Trade-off between genetic variation and ecological adaptation of metallicolous and non-metallicolous Noccaea and Thlaspi species. Environ. Exp. Bot. 96, 1–10. https://doi.org/10.1016/J.ENVEXPBOT.2013.08.002.

Majumdar, S., Ma, C., Villani, M., Zuverza-Mena, N., Pagano, L., Huang, Y., Zappettini, A., Keller, A.A., Marmiroli, N., Dhankher, O.P., White, J.C., 2019. Surface coating determines the response of soybean plants to cadmium sulfide quantum dots. NanoImpact 14, 100151. https://doi.org/10.1016/J.IMPACT.2019.100151.

Małgorzata, P., Paweł, K., Iwona, M.L., Brzostek, T., Andrzej, P., 2020. Glutamatergic dysregulation in mood disorders: opportunities for the discovery of novel drug targets. Expert Opin. Ther. Targets 24, 1187–1209. https://doi.org/10.1080/14728222.2020.1836160.

Marmiroli, M., Lepore, G.O., Pagano, L., D'Acapito, F., Gianoncelli, A., Villani, M., Lazzarini, L., White, J.C., Marmiroli, N., 2020. The fate of CdS quantum dots in plants as revealed by extended X-ray absorption fine structure (EXAFS) analysis. Environ. Sci. Nano 7, 1150–1162. https://doi.org/10.1039/c9en01433k.

Marmiroli, M., Maestri, E., Pagano, L., Robinson, B.H., Ruotolo, R., 2019. Toxicology assessment of engineered nanomaterials: innovation and tradition. Expo. Eng. Nanomater. Environ. 209–234. https://doi.org/10.1016/B978-0-12-814835-8.00008-X.

Marmiroli, M., Pagano, L., Sardaro, M.L.S., Villani, M., Marmiroli, N., 2014. Genome-wide Approach in Arabidopsis thaliana to Assess the Toxicity of Cadmium Sulfide Quantum Dots. https://doi.org/10.1021/es404958r.

Marmiroli, N., 2007. Geneticvariability and genetic engineering in phytoremediation. Advanced Science and Technology for Biological Decontamination of Sites Affected by Chemical and Radiological Nuclear Agents. Springer Netherlands, Dordrecht, pp. 89–108 https://doi.org/10.1007/978-1-4020-5520-1_6.

Marmiroli, N., Marmiroli, M., Maestri, E., 2006. Phytoremediation and phytotechnologies: a review for the present and the future. Soil and Water Pollution Monitoring, Protection and Remediation. Springer Netherlands, Dordrecht, pp. 403–416 https://doi.org/10.1007/978-1-4020-4728-2_26.

Marmiroli, McCutcheon, 2003. Making phytoremediation a successful technology. Phytoremediation. John Wiley & Sons, Inc., Hoboken, NJ, USA, pp. 85–119 https://doi.org/10.1002/047127304X.ch3.

Marques, A.P.G.C., Rangel, A.O.S.S., Castro, P.M.L., 2009. Remediation of heavy metal contaminated soils: phytoremediation as a potentially promising clean-up technology. Crit. Rev. Environ. Sci. Technol. 39, 622–654. https://doi.org/10.1080/10643380701798272.

McGrath, S.P., Lombi, E., Gray, C.W., Caille, N., Dunham, S.J., Zhao, F.J., 2006. Field evaluation of Cd and Zn phytoextraction potential by the hyperaccumulators Thlaspi caerulescens and Arabidopsis halleri. Environ. Pollut. 141, 115–125. https://doi.org/10.1016/J.ENVPOL.2005.08.022.

McGrath, S.P., Zhao, F.-J., 2003. Phytoextraction of metals and metalloids from contaminated soils. Curr. Opin. Biotechnol. 14, 277–282. https://doi.org/10.1016/S0958-1669(03)00060-0.

McIntyre, T., 2003. Phytoremediation of Heavy Metals from Soils. Springer, Berlin, Heidelberg, pp. 97–123 https://doi.org/10.1007/3-540-45991-X_4.

Miralles, P., Church, T.L., Harris, A.T., 2012. Toxicity, uptake, and translocation of engineered nanomaterial in vascular plants. Environ. Sci. Technol. 46, 9224–9239.

Mišljenović, T., Jovanović, S., Mihailović, N., Gajić, B., Tomović, G., Baker, A.J.M., Echevarria, G., Jakovljević, K., 2020. Natural variation of nickel, zinc and cadmium (hyper)accumulation in facultative serpentinophytes Noccaea kovatsii and N. praecox. Plant Soil 447, 475–495. https://doi.org/10.1007/S11104-019-04402-5/TABLES/8.

Oomen, R.J.F.J., Wu, J., Lelièvre, F., Blanchet, S., Richaud, P., Barbier-Brygoo, H., Aarts, M.G.M., Thomine, S., 2009. Functional characterization of NRAMP3 and NRAMP4 from the metal hyperaccumulator Thlaspi caerulescens. New Phytol. 181, 637–650. https://doi.org/10.1111/J.1469-8137.2008.02694.X.

Ovečka, M., Lang, I., Baluška, F., Ismail, A., Illeš, P., Lichtscheidl, I.K., 2005. Endocytosis and vesicle trafficking during tip growth of root hairs. Protoplasma 226, 39–54.

Pagano, L., Maestri, E., Caldara, M., White, J.C., Marmiroli, N., Marmiroli, M., 2018a. Engineered nanomaterial activity at the organelle level: impacts on the chloroplasts and mitochondria. ACS Sustain. Chem. Eng. 6, 12562–12579. https://doi.org/10.1021/acssuschemeng.8b02046.

Pagano, L., Maestri, E., White, J.C., Marmiroli, N., Marmiroli, M., 2018b. Quantum dots exposure in plants: minimizing the adverse response. Curr. Opin. Environ. Sci. Health 6, 71–76. https://doi.org/10.1016/J.COESH.2018.09.001.

Pagano, L., Maestri, E., White, J.C., Marmiroli, N., Marmiroli, M., 2018c. Quantum dots exposure in plants: minimizing the adverse response. Curr. Opin. Environ. Sci. Health 6, 71–76. https://doi.org/10.1016/J.COESH.2018.09.001.

Pagano, L., Pasquali, F., Majumdar, S., De la Torre-Roche, R., Zuverza-Mena, N., Villani, M., Zappettini, A., Marra, R.E., Isch, S.M., Marmiroli, M., Maestri, E., Dhankher, O.P., White, J.C., Marmiroli, N., 2017. Exposure of Cucurbita pepo to binary combinations of engineered nanomaterials: physiological and molecular response. Environ. Sci. Nano 4, 1579–1590. https://doi.org/10.1039/C7EN00219J.

Pagano, L., Servin, A.D., De La Torre-Roche, R., Mukherjee, A., Majumdar, S., Hawthorne, J., Marmiroli, M., Maestri, E., Marra, R.E., Isch, S.M., Dhankher, O.P., White, J.C., Marmiroli, N., 2016. Molecular response of crop plants to engineered nanomaterials. Environ. Sci. Technol. 50, 7198–7207. https://doi.org/10.1021/acs.est.6b01816.

Pence, N.S., Larsen, P.B., Ebbs, S.D., Letham, D.L.D., Lasat, M.M., Garvin, D.F., Eide, D., Kochian, L.V., 2000. The molecular physiology of heavy metal transport in the Zn/Cd hyperaccumulator Thlaspi caerulescens. Proc. Natl. Acad. Sci. 97, 4956–4960. https://doi.org/10.1073/PNAS.97.9.4956.

Psaras, G.K., Manetas, Y., 2001. Nickel localization in seeds of the metal hyperaccumulator Thlaspi pindicum Hausskn. Ann. Bot. 88, 513–516. https://doi.org/10.1006/ANBO.2001.1470.

Reeves, R.D., Schwartz, C., Morel, J.L., Edmondson, J., 2001. Distribution and metal-accumulating behavior of Thlaspi caerulescens and associated metallophytes in France. Int. J. Phytoremediation 3, 145–172. https://doi.org/10.1080/15226510108500054.

Rigola, D., Fiers, M., Vurro, E., Aarts, M.G.M., 2006. The heavy metal hyperaccumulator Thlaspi caerulescens expresses many species-specific genes, as identified by comparative expressed sequence tag analysis. New Phytol. 170, 753–766. https://doi.org/10.1111/j.1469-8137.2006.01714.x.

Ruotolo, R., Pira, G., Villani, M., Zappettini, A., Marmiroli, N., 2018. Ring-shaped corona proteins influence the toxicity of engineered nanoparticles to yeast. Environ. Sci. Nano 5, 1428–1440. https://doi.org/10.1039/C7EN01226H.

Servin, A.D., Castillo-Michel, H., Hernandez-Viezcas, J.A., Corral Diaz, B., Peralta-Videa, J.R., Gardea-Torresdey, J.L., 2012. Synchrotron micro-XRF and micro-XANES confirmation of the uptake and translocation of TiO2 nanoparticles in cucumber (Cucumis sativus). Plants. https://doi.org/10.1021/es300955b.

Servin, A.D., Pagano, L., Castillo-Michel, H., De la Torre-Roche, R., Hawthorne, J., Hernandez-Viezcas, J.A., Loredo-Portales, R., Majumdar, S., Gardea-Torresday, J., Dhankher, O.P., White, J.C., 2017. Weathering in soil increases nanoparticle CuO bioaccumulation within a terrestrial food chain. Nanotoxicology 11, 98–111. https://doi.org/10.1080/17435390.2016.1277274.

Singh, R.P., Handa, R., Manchanda, G., 2021. Nanoparticles in sustainable agriculture: an emerging opportunity. J. Control. Release 329, 1234–1248. https://doi.org/10.1016/j.jconrel.2020.10.051.

Tan, W., Du, W., Barrios, A.C., Armendariz, R., Zuverza-Mena, N., Ji, Z., Chang, C.H., Zink, J.I., Hernandez-Viezcas, J.A., Peralta-Videa, J.R., Gardea-Torresdey, J.L., 2017. Surface coating changes the physiological and biochemical impacts of nano-TiO2 in basil (Ocimum basilicum) plants. Environ. Pollut. 222, 64–72. https://doi.org/10.1016/j.envpol.2017.01.002.

Usman, M., Farooq, M., Wakeel, A., Nawaz, A., Cheema, S.A., Rehman, H.ur, Ashraf, I., Sanaullah, M., 2020. Nanotechnology in agriculture: current status, challenges and future opportunities. Sci. Total Environ. 721, 137778. https://doi.org/10.1016/j.scitotenv.2020.137778.

Villani, M., Calestani, D., Lazzarini, L., Zanotti, L., Mosca, R., Zappettini, A., 2012. Extended functionality of ZnO nanotetrapods by solution-based coupling with CdS nanoparticles. J. Mater. Chem. 22, 5694. https://doi.org/10.1039/c2jm16164h.

Visioli, G., Pirondini, A., Malcevschi, A., Marmiroli, N., 2010a. Comparison of protein variations in Thlaspi caerulescens populations from metalliferous and non-metalliferous soils. Int. J. Phytoremediation 12, 805–819. https://doi.org/10.1080/15226510903353138.

Visioli, G., Pirondini, A., Malcevschi, A., Marmiroli, N., 2010b. Comparison of protein variations in Thlaspi caerulescens populations from metalliferous and non-metalliferous soils. Int. J. Phytoremediation 12, 805–819. https://doi.org/10.1080/15226510903353138.

Volkov, Y., 2015. Quantum dots in nanomedicine: recent trends, advances and unresolved issues. Biochem. Biophys. Res. Commun. 468, 419–427. https://doi.org/10.1016/J.BBRC.2015.07.039.

Zayed, A., Gowthaman, S., Terry, N., 1998. Phytoaccumulation of trace elements by wetland plants: I. duckweed. J. Environ. Qual. 27, 715. https://doi.org/10.2134/jeq1998.00472425002700030032x.

Zemanová, V., Pavlík, M., Pavlíková, D., Hnilička, F., Vondráčková, S., 2016. Responses to Cd stress in two Noccaea species (Noccaea praecox and Noccaea caerulescens) originating from two contaminated sites in Mežica, Slovenia and Redlschlag, Austria. Arch. Environ. Contam. Toxicol. 70, 464–474. https://doi.org/10.1007/s00244-015-0198-8.

Zhao, F.J., Jiang, R.F., Dunham, S.J., McGrath, S.P., 2006. Cadmium uptake, translocation and tolerance in the hyperaccumulator Arabidopsis halleri. New Phytol. 172, 646–654. https://doi.org/10.1111/J.1469-8137.2006.01867.X.

Zuverza-Mena, N., White, J.C., 2018. Engineered nanomaterials in terrestrial systems: interactions with co-existing contaminants and trophic transfer. Curr. Opin. Environ. Sci. Health 6, 60–65. https://doi.org/10.1016/J.COESH.2018.08.003.